Egusphere-2024-1696

Quaternary surface ruptures of the inherited mature Yangsan Fault: implications for intraplate earthquakes in Southeastern Korea

Comment	Change made
Reviewer 2	
Major comments	
Based on the current quality of this manuscript entitled “Quaternary surface ruptures of the inherited mature Yangsan fault: implications for intraplate earthquakes in Southeastern Korea”, it is unsuitable to accept this current manuscript; a thorough revision should be made. Thus, I recommend a major revision before publication. The general comments are as follows:	Thank you for your time and effort in offering us constructive feedback. We did our best to digest and incorporate the valuable comments. We are sure that the current manuscript has been greatly improved to meet the journal's standards and quality.
The northern segment of the Yangsan fault is a right-lateral strike-slip fault. If there are any associated offset channels, terraces, or alluvial fans, the authors should provide some figures to show these offset landforms. The authors should add a tectonic geomorphic map for each trench site, showing the offset landforms, sedimentary environment, etc., to give readers more comprehensive information about the trench location.	Thanks. We found several geomorphic offsets along the fault trace, so we added geomorphic information in chapter 2.2, 3.1, 4.1, and Appendix A. ***Line 113-120*** **2.2 Geological settings of the Byeokgye section of the Yangsan Fault** The Northern Yangsan Fault, located north of Gyeongju at the junction of, the Ulsan and Yangsan Faults, has documented several Quaternary surface ruptures (Fig. 1b). These surface ruptures caused offsets in alluvial fans, river terraces, and deflected rivers with dextral displacements of 0.43-2.82 km (Kyung, 2003; Choi et al., 2012; Lee et al., 2019; Han et al., 2021; Ko et al., 2022; Lee et al., 2022; Lee, 2023). Recent significant earthquakes in Pohang and Gyeongju further underscore the seismic activity of this region. The Byeokgye section, which crosses Gyeongju and Pohang, is located in the southern part of the Northern Yangsan Fault, adjacent to the Yugye and Bangok sites to the north. In contrast, no Quaternary surface rupture has been identified in the Angang area to the south. ***Line 152*** **3.1 Fault surface rupture tracking and trench siting** The detailed topography of the study area is described in Appendix A. ***Line 255-259*** **4.1.1 Trench 1** It is located on the main lineament, approximately 1 km north of the Byeokgye site (Fig. 2c), within a cultivated field where a narrow 50 m wide N-S trending valley and a 20 m wide NE-trending valley meet, through which the main lineament passes. To the east of Trench 1, a NE-trending ridge develops, although this is currently difficult to identify due to human modification, while to the west, a hill with a N-S trending ridge is formed (Fig. A2). Fault scarps are distinctly visible along the main lineament, both to the south and north of Trench 1, with small fluvial and colluvial deposits observed on the surface. ***Line 316-320*** **4.1.2 Trench 2** Trench 2 is located on the main lineament 0.8 km north of Trench 1 (Fig. 2c), within a colluvial area where fault scarp extend continuously along the main lineament to the south and north. Just north of Trench 2, the transition to an alluvial fan is clearly visible where the mountain ridge meets the main lineament. The 25-m wide valley surface contains partially developed colluvial sediments and deposits from small streams and gullies.

	Line 357-361 **4.1.3 Trench 3** Trench 3 is located on the main lineament extending 1.7 km north of the Trench 2 (Fig. 2c), within a cultivated field next to a wide road at the mouth of a broad basin. Fault scarps along the main lineament extend both south and north of the Trench 3. This trench marks the northernmost point where the transition to the alluvial fan is observed where the mountain ridge meets the main lineament; beyond this point, fault scarps continue to develop on the alluvial fan surface. ***Line 388-392*** **4.1.4 Trench 4** Trench 4 is situated on a NE-striking eastern branch lineament from the main lineament, which stretches 2.8 km north of the Trench 3 (Fig. 2c). South of Trench 4, a continuous dextrally deflected stream follows the branching lineament, with smaller displacements identified further north. Trench 4 lies at the edge of an alluvial fan near a hillslope, with two features separated by a stream. ***Line 415-417*** **4.1.5 Trench 5** Trench 5 is located 40 m north of Trench 4. Because of its proximity, Trench 5 shares identical topographic characteristics with Trench 4, except that it lies on the margins of a hillslope instead of on an alluvial fan. ***Line 627-657*** **Appendix A. Geomorphic map of study area** The topography of the study area in Ha et al. (2022) is summarized as follows: The study area's topography is divided into a lowland area to the west and a mountainous region to the east (Fig. A1). The eastern mountains, the ridges extending from the summit are cut off by a lineament heading west, which influences the drainage system, with streams flowing from the high elevations east to the west. Alluvial fans, formed from sediments from the eastern mountains, are found at the base of the slopes. Twelve lineaments are identified, with the main lineament, which extends for 7.6 km, displaying high activity through the northern part of the Byeokgye site. Subsidiary high-activity lineaments and low-activity lineaments, mainly following N–S or NNE directions, are present, though many are valleys formed by erosion rather than rupturing. The main lineament exhibits continuous fault scarps and deflected streams, with reservoirs often located along it due to impermeable fault gouges that enable water storage. Topographic analysis revealed fault scarps, knickpoints, and displacement features along the main lineament, particularly visible in LiDAR data. Fault scarps are continuously and distinctly visible in the main lineament of the southern region (Fig. A2). In the cross-section, the fault scarps are recognized as knickpoints, and on the topographical map, the ridges on the east side of the lineament are cut by the surface rupture and merged with the alluvial fans. The main lineament of the northern region is identified as a linear arrangement of deflected streams and fault scarps (Fig. A3). Unlike in the south, the fault scarps in the north show surface uplift estimated at a vertical offset of between 2–4.2 m of the same alluvial fan surface cross-section. Differences between the southern and northern regions are observed, with the north showing vertical offsets of 2–4.2 m and more pronounced faulting. The horizontal offsets calculated based on the three deflected streams are 92 m, 98 m, and 150 m. The tendency for the offset to decrease as the distance from the main lineament increases indicates that the fault offset branching from the main surface rupture gradually decreases.

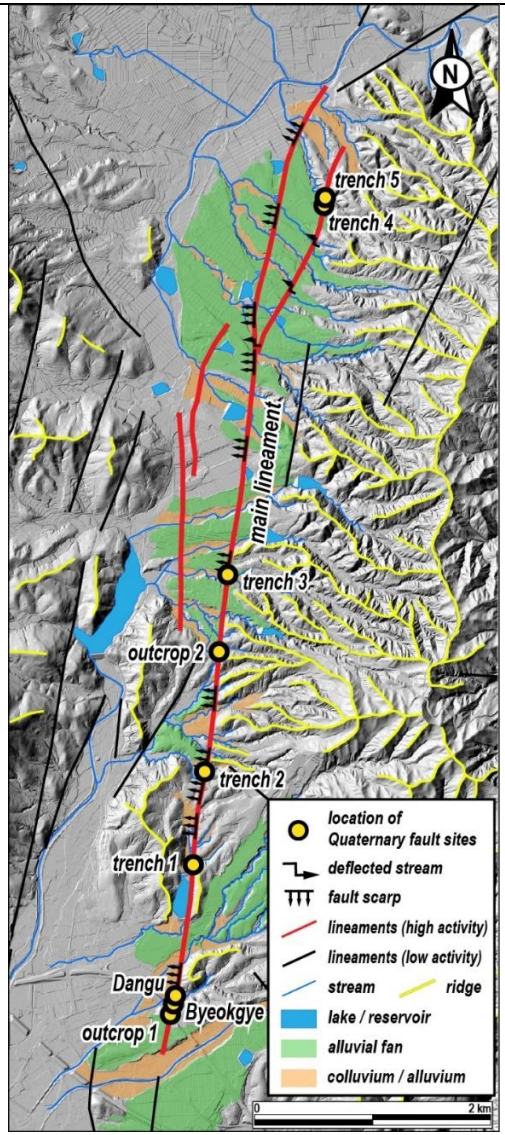

Figure A1: The geomorphic map of the study area (modified from Ha et al., 2022).

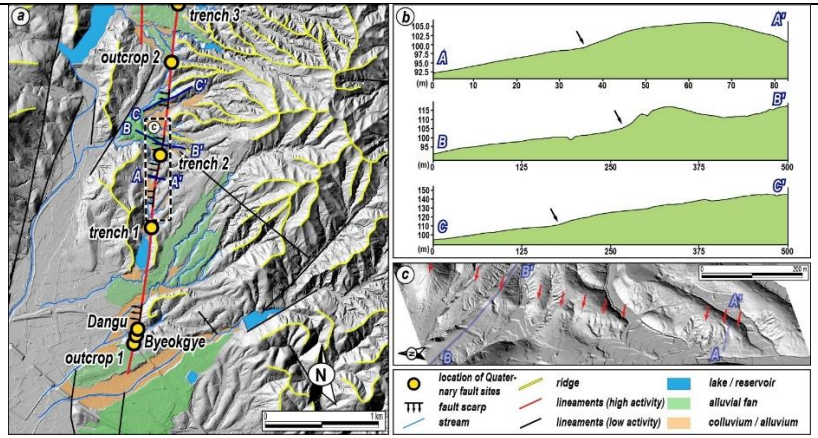

Figure A2: (a) A detailed topographic map of the southern region. (b) Topographic profiles along the main lineament (blue line in (a)) crossing the fault scarps. Black arrows mark knickpoints identified as fault scarps. (c) A 3D hillshade image. The red arrows highlight the fault scarp, which is clearly visible to the unaided eye.

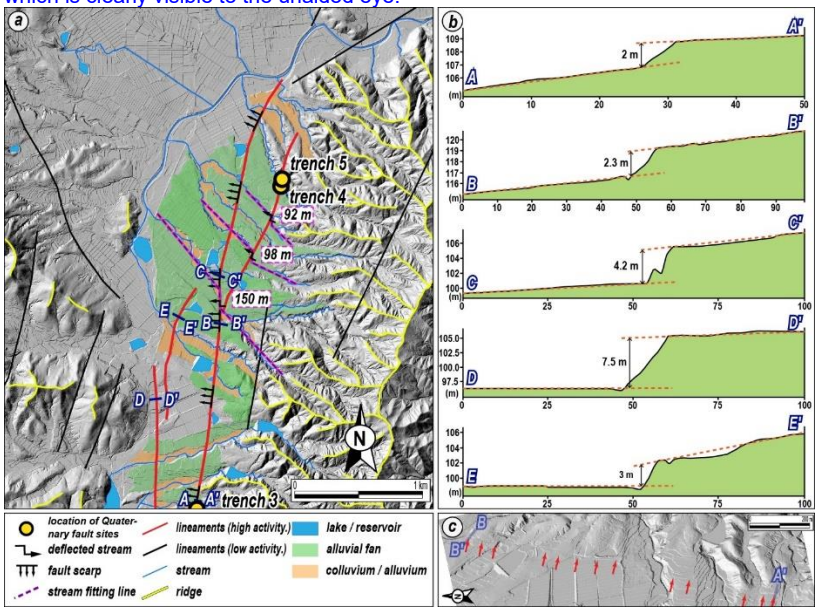

Figure A3: (a) A detailed topographic map of the northern region. An NNE lineament branching off from the main lineament is shown by the dextrally deflected stream. (b) Topographic profiles along the line (blue line in (a)) crossing the fault scarps. Fault scarps in the northern region are evident due to the elevation difference in the alluvial fan surfaces. (c) A 3D hillshade image. Red arrows highlight the fault scarp.

It is suggested that the sample number should be marked on the trench logs to help readers judge the sample location.	Thanks, we added the sample number and each dating result in the trench logs.

Fig. 3

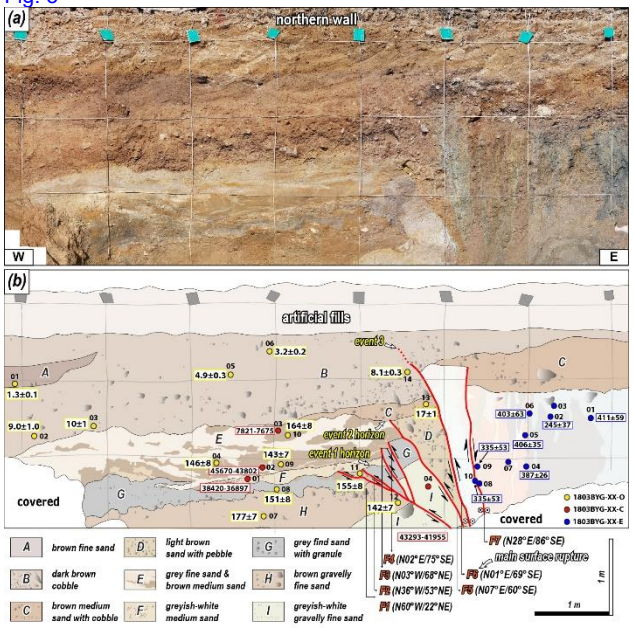

Fig. 4

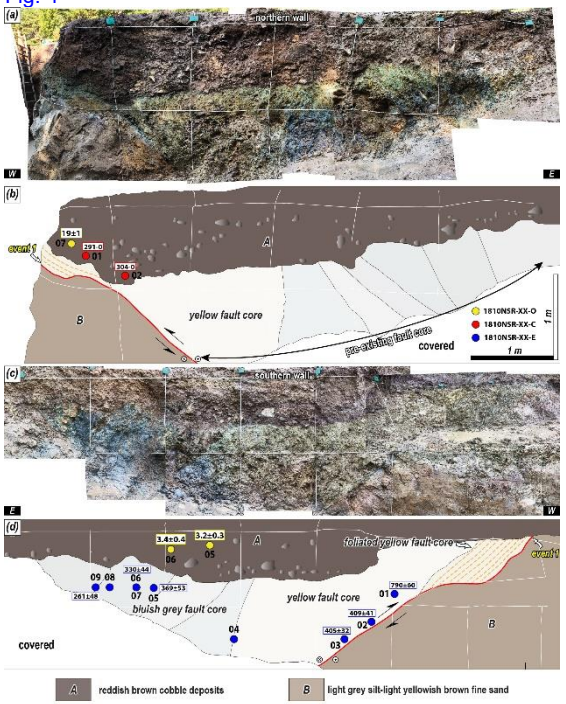

Fig. 5

Fig. 6

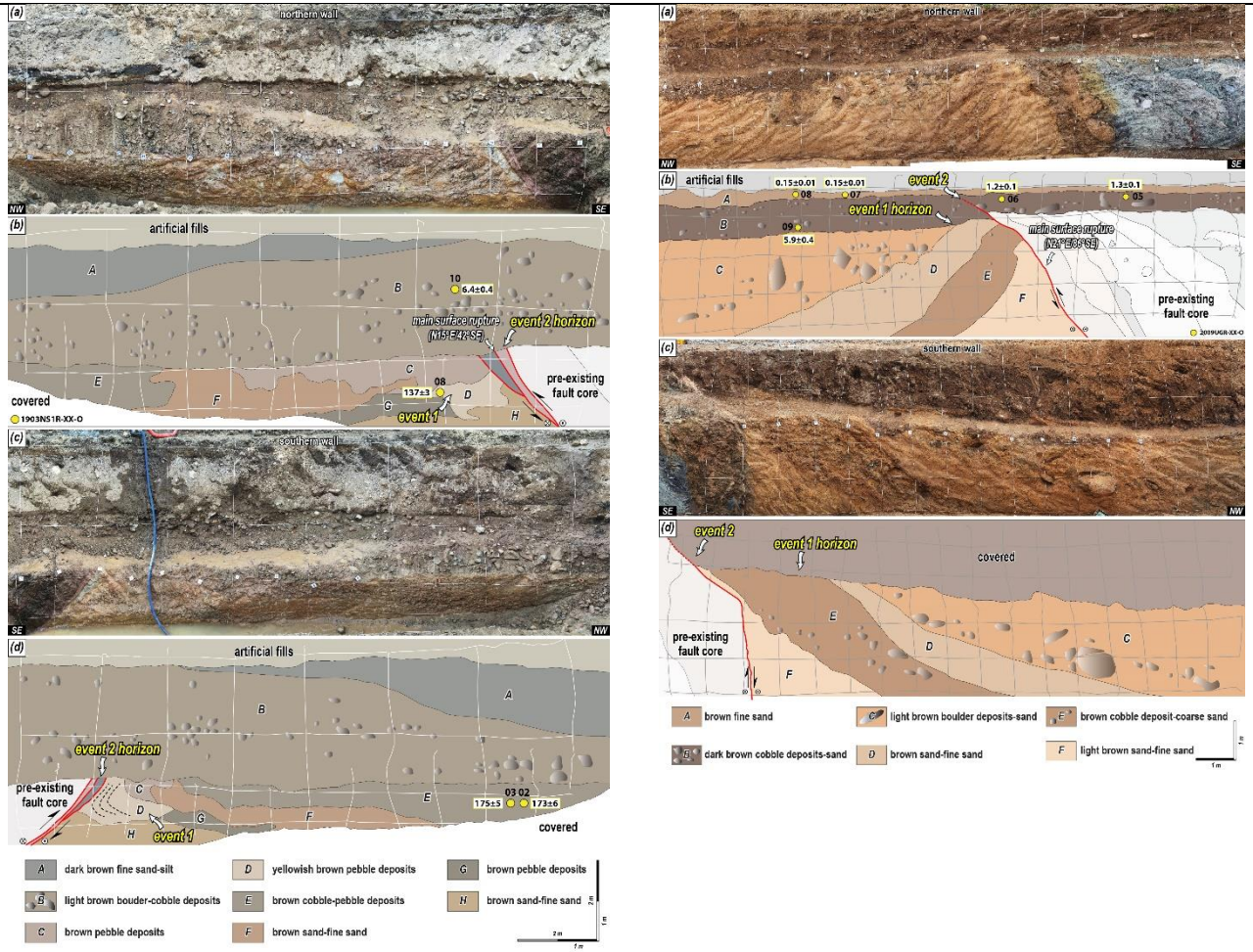
(a)
northern wall
NW
SE
(b)
artificial fills
A
B
10
6.4±0.4
main surface rupture
(N15°E/43°SE)
event 2 horizon
C
E
F
G
D
H
137±3
08
event 1
pre-existing
fault core
covered
1903NS1R-XX-O
(c)
southern wall
SE
NW
(d)
artificial fills
A
B
event 2 horizon
pre-existing
fault core
C
D
G
H
event 1
E
F
03 02
175±5
173±6
covered
A dark brown fine sand-silt
B light brown bouder-cobble deposits
C brown pebble deposits
D yellowish brown pebble deposits
E brown cobble-pebble deposits
F brown sand-fine sand
G brown pebble deposits
H brown sand-fine sand
2 m
1 m
(a)
northern wall
NW
SE
(b)
artificial fills
0.15±0.01
0.15±0.01
08
07
event 2
1.2±0.1
06
1.3±0.1
05
A
B
09
5.9±0.4
event 1 horizon
main surface rupture
(N4°E/68°SE)
C
D
E
F
pre-existing
fault core
2019UGR-XX-O
(c)
southern wall
SE
NW
(d)
event 2
event 1 horizon
covered
pre-existing
fault core
E
D
C
F
A brown fine sand
C light brown boulder deposits-sand
E brown cobble deposit-coarse sand
B dark brown cobble deposits-sand
D brown sand-fine sand
F light brown sand-fine sand
1 m

Fig. 7

	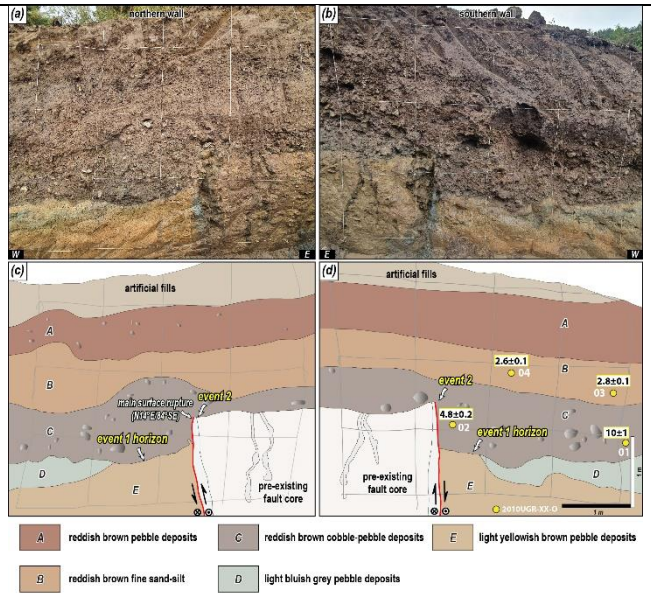
It is recommended to provide locally enlarged photos of the sampled strata to distinguish the characteristics of the sedimentary strata. Because the reliability of OSL dating results is related to the sedimentary characteristics. Based on the photos currently presented, the sorting and rhythmicity of the strata are both poor, which is unsuitable for OSL dating.	Thanks for the constructive comment. We understand what the reviewer tried to mean, but the reliability of luminescence dating results may not be necessarily related to depositional environments (or processes). As the reviewer may know, there have been lots of published papers where luminescence dating results were used as useful age controls for age-unknown sediments that had formed in various environments (e.g., glaciofluvial, alluvial fan, marine, and what not). Having said that, we are well aware that the physical characteristics of luminescence signals (quartz OSL signal, in particular) can be controlled by sedimentation processes. For instance, in general, as the transportation distance of mineral grains increases, the luminescence signal properties become more suitable for reliable age estimation; It is well known that the fast quartz OSL signal, which is the main target signal for quartz OSL dating, become prominent with the increase in transportation distance. Besides, it is also true that the well-sorted sediments, which are presumed to be of uniform natural radioactivity, put much less complexity in environmental dose rate estimation than poorly sorted ones. As represented in Appendix D, the quartz OSL signals for all the samples appear to be dominated by the fast OSL signal component. Further, both quartz OSL and K-feldspar pIRIR$_{225}$ signals passed through the acceptance criteria of the SAR protocol (e.g., recycling ratio within 10% of unity, recuperation less than 5 % of the natural signal intensity etc.). As depicted with probability density plots showing negligible skewness (Figure E1), we could not detect any clear evidence of detrimental effects from substantial incomplete bleaching of luminescence signals at deposition, although the luminescence signal measurements were performed using multiple grain single aliquots (“3 mm” aliquots). From the perspective of dose rate estimation, most samples were collected from homogeneous sandy layers, at least ~ 30 cm away from pebble clasts. Where it was unavoidable to take samples from pebbly sediments, we separately collected representative sediment samples, mixture of sands and pebbles, and pulverized them for homogenization. Then these were used for gamma measurements (environmental dose rate estimation). Therefore, we consider that the presence of pebble clasts, together with sandy grains, did not give rise to substantial luminescence age bias. Based on these, there is no reason to doubt the reliability of the luminescence ages of the samples, particularly with regard to the degree of sorting, and we conclude that the luminescence ages presented here can be given credence, at least at this stage of investigation.

There is significant uncertainty in the calculation method of slip rate in the text, which is also pointed out by the author. The best way to limit the slip rate of strike-slip faults is to use the displaced geomorphic surface to constrain the slip rate. It is suggested that the author can do such work in this area in the future.	That's a great comment. To best address your comment, we have replaced true displacement with horizontal displacement, presented slip rate and displacement based on horizontal as well, and clearly stated the uncertainties and limitations associated with this in strike-slip faulting settings. ***Line 224-250*** **3.4 Displacement and earthquake magnitude estimation** The slickenlines of the main surface rupture and the vertical separation of the Quaternary sediments in the trench wall are used to determine the horizontal displacement of the MRE and the displacement per event. In general, for strike-slip faults like the study area, horizontal displacements must be obtained from 3D trenches or from topography that preserves the displacements almost intact (e.g., Kim et al., 2024; Naik et al., 2024). Using only 2D trenches to obtain displacements or slip rates is uncertain because the sedimentary layers are unlikely to have recorded all earthquakes. Furthermore, deriving the horizontal displacement is challenging when exposed walls are inclined, markers are inclined, or the slip sense is not purely dip-slip or strike-slip (which is almost always the case). In addition, displacements based on fragmentary information, such as bedrock separation and thickness of Quaternary sediments, can be over- or underestimated by fault slip motion and the possibility of paleo-topographic relief cannot be ignored. Despite these uncertainties, fault displacement is a necessary factor in earthquake magnitude estimation and key paleoseismological information, and the displacement obtained from the 2D trench can be used as a minimum value; therefore, the process of collecting or estimating fault displacement is indispensable in paleoseismology. Therefore, correlations based on vertical separation, marker dip angle, angle of slope wall, fault dip angle, rake of slickenline, etc. are important for estimating the horizontal displacement of a fault (Fig. B1; Xu et al., 2009; Jin et al., 2013; Lee et al., 2017; Gwon et al., 2021). The method of using their relationship to find the horizontal displacement is described in detail in Appendix B. Variables used for earthquake magnitude estimation include average displacement (Kanamori, 1977), maximum displacement (MD; Bonilla et al., 1984; Wells and Coppersmith, 1994), surface rupture length (Bonilla et al., 1984; Khromovskikh, 1989; Wells and Coppersmith, 1994), rupture area (Wells and Coppersmith, 1994), and surface rupture length × MD (Bonilla et al., 1984; Mason, 1996). However, in Korea, where rupture traces are difficult to find, it is difficult to use surface rupture length or rupture area owing to large uncertainties. Thus, we used MD (horizontal displacement), which is relatively easy to obtain from outcrops and trenches and more reliable. Many previous studies within intraplate have applied the empirical relationship of the MD-moment magnitude (M_w) presented by Wells and Coppersmith (1994) (e.g., Patyniak et al., 2017 in Kyrgyzstan; Suzuki et al., 2020 in Mongolia; Je et al., 2024., in China). We also estimated the maximum earthquake magnitude by applying the MD obtained from the trench to the empirical formula. The rake of slickenlines on the Quaternary slip surface that underwent faulting averages 20° and strike-slip motion is dominant; therefore, we used a corresponding strike-slip fault type M_w-MD empirical relationship. ***Line 450-468*** **4.4 Displacement and earthquake magnitude estimation** The results calculated using the marker, vertical separation of each trench, and Eq. (B1) are listed in Table 5. In the previous study by Lee et al. (2016), the horizontal displacement of the MRE at the Dangu site is determined to be 2.55 m. For each surface rupturing event in Trench 1, the horizontal displacement per event according to the event horizon is 0.9–1.05 m, and the horizontal displacement of the MRE is 1.72 m. Using the bedrock and Quaternary sediments unconformity identified by corings in Trench 2 as a marker, the cumulative horizontal displacement is 76 m. The MRE cutting the colluvial wedge in Trench 3 has a horizontal displacement of 2.85 m. However, when considering the overall interpretation, only the MRE and AE, but not the PE, are recognized in Trench 3 (Figs. 5 and 9). The displacement cutting the colluvial wedge likely reflects the displacement of the missing PE as well as the MRE, which is supported by the long interval between the wedge (unit D) and the deposit covering the wedge (unit B). Thus, it is reasonable to exclude the calculated displacement as it is unlikely to be the displacement of the MRE. The horizontal displacement of the MRE in Trench 4 and 5 are 0.82 m and 2.21 m, respectively, using the lower boundary of units B and C as markers. Combining the results from each trench, the horizontal displacement of MRE in the study area is 0.82–2.55 m and the cumulative horizontal displacement is 76 m. The horizontal displacement per event is similar, between 0.9–1.05 m for PE and AE (event 1, 2), but the trench shows a higher displacement for the MRE (event 3). We estimated the maximum earthquake magnitude by applying the MD (horizontal displacement: 0.82-2.55 m) of the MRE, resulting in a maximum magnitude estimate 6.7–7.1. Seismic SSDs such as the 20-50 clastic dike and 30 cm ball-and-pillow structure observed in the exposed wall (units E and G in Trench 1; unit F in Trench 3), serve as indirect evidence indicating an earthquake of at least magnitude 5.5 (Atkinson et al., 1984).

Table 5. Fault displacement of study area

		S_v (m)	α (°)	γ (°)	S_t (m)	**S_h (m)**
Dangu[a]	MRE (event 3)	0.67	79	15	2.64	**2.55**
	Marker	Unit D				
Trench 1[b]	MRE (event 3)	0.49	69	17	1.8	**1.72**
	Marker	Unit C				
	PE (event 2)	0.31	75	17	1.1	**1.05**
	Marker	Unit G				
	AE (event 1)	0.22	53	17	0.94	**0.9**
	Marker	Unit H				
Trench 2	Cumulative displacement	34	38	36	94	**76**
	Marker	Quaternary deposits thickness				
Trench 3	MRE (event 3)	1.1	42	30	3.29	**2.85**
	Marker	Unit D				
Trench 4	MRE (event 3)	0.25	86	17	0.86	**0.82**
	Marker	Unit B				
Trench 5	MRE (event 3)	0.8	84	20	2.35	**2.21**
	Marker	Unit C				

Line 493-518

5.1.2 Quaternary slip rate and recurrence interval

The slip rate is an expression of the average displacement of a fault over a certain period, which numerically shows how quickly energy (stress) accumulates in a fault zone and is used as an important input parameter in seismic hazard assessment (Liu et al., 2021). The horizontal slip rate in the study area is calculated based on the earthquake timing and horizontal displacement of each trench. We calculated slip rates from three trenches spanning different periods: Late Pleistocene to Holocene (Trench 1), Quaternary (Trench 2), and Middle Pleistocene to Holocene (Trench 3). In Trench 1, we derived a slip rate of 0.12-0.14 mm/yr based on the horizontal displacement of event 3 (MRE) of 1.72 m and the 13.8±1.2 ka time interval between events 3 and 2 (time gap between units B and C; Table 1). For Trench 2, borehole data revealed a slip rate of 0.02-0.03 mm/yr, calculated from the cumulative horizontal displacement of 76 m and the cosmogenic ^{10}Be-^{26}Al isochron burial age of 2.87±0.59 Ma from the lowermost Quaternary deposits. In Trench 3, we calculated a slip rate of 0.02 mm/yr using the 2.85 m horizontal displacement of the event that cut the colluvial wedge (unit D) and the 130.6±3.4 ka time interval between events (time gap between units B and D).

Considering the age of the deposits, the slip rate of 0.12-0.14 mm/yr from Trench 1 represents movement during the Holocene, while the rates from Trenches 2 and 3 may represent cumulative slip rate (0.02 mm/yr) throughout the Quaternary. As noted in the method section (3.3), there are uncertainties in obtaining slip rates from 2D trenches alone on strike-slip faults such as the study area. In particular, the discontinuous distribution of Quaternary sediments may have led to a misestimation of the slip rate. There are two distinct types of sediments in the trench wall: (1) light brown, relatively coarse-grained sediments of mid-to-late Pleistocene age, which tend to be tilted in the vicinity of the surface rupture, and (2) dark brown, relatively coarse-grained, nearly horizontal Holocene sediments (Table 1, Figs. 3-7). The exact absolute time interval between these two deposits is unknown; however, there is unconformity, and the MRE mostly cut Holocene sediments (<10,000 years). A depositional gap, such as an unconformity, causes earthquake records to be missed during that time, leading to a misestimation of the slip rate. For this reason, in strike-slip fault settings, 3D trenching should be used because the slip rate using displacement from 2D trenches is

underestimated compared to the slip rate using topography, which preserves most of the displacement. The slip rates in this study (0.12-0.14 mm/yr) are lower compared to the slip rates derived from the topography and 3D-trench reported in the study area of 0.38-0.57, 0.5 mm/yr, respectively (Kim et al., 2024; Naik et al., 2024). Nevertheless, the slip rates in our study are meaningful as a minimum value that establishes a lower boundary for the slip rates in the study area.

Line 659-672

Appendix B. Calculation of horizontal displacement

The horizontal displacement (S_h) can be calculated using a trigonometric function that considers the vertical displacement (S_v), fault dip angle (α), rake (γ), true displacement (S_t) and their relationships (Fig. B1; Eq. B1). Assume that the attitude of the marker in the exposed wall at each trench is nearly horizontal in three dimensions and the angle (β) of the exposed wall is nearly vertical, then the two factors are perfectly horizontal and vertical, respectively. Thus, the vertical separation (S_{vm}) and vertical displacement (S_v) measured in the exposed wall are equal. Therefore,

$$S_{vm} = S_v, S_m = \frac{S_v}{\sin\alpha}, S_t = \frac{S_m}{\sin\gamma}, S_h = \cos\gamma * S_t \quad \text{(B1)}$$

We calculate horizontal displacement (S_h) using Eq. (B1) for vertical separation (S_{vm}) of the marker measured in the exposed wall, as shown in Table 5.

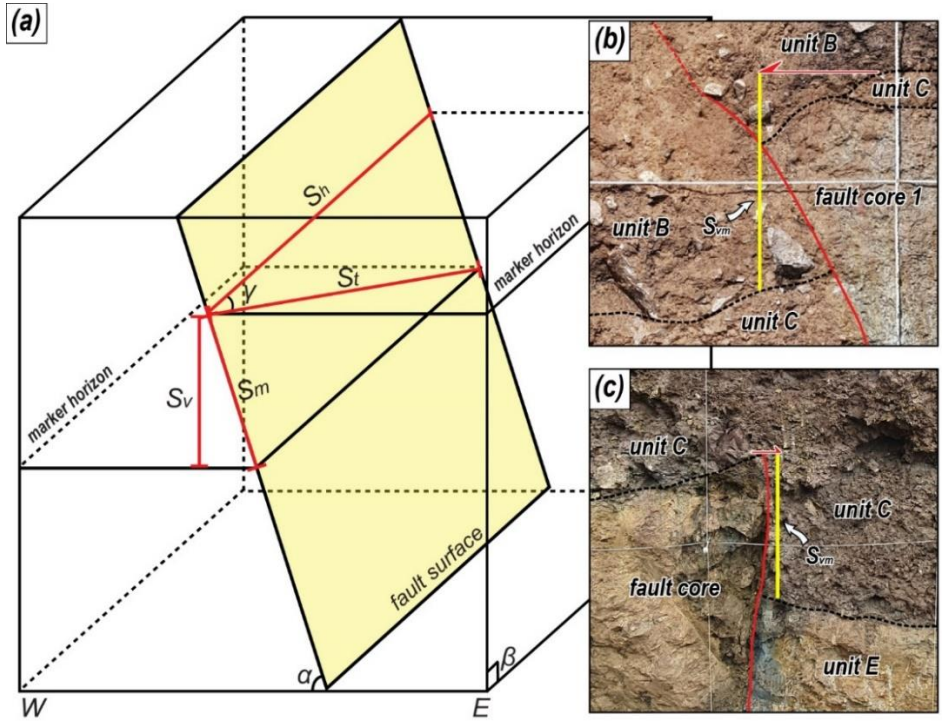

Figure B1: (a) Schematic diagram showing how to calculate true displacement. S_h: horizontal displacement S_t: true displacement, S_v: vertical displacement, S_m: dip separation, α: dip of fault surface, β: dip of cut slope, γ: rake of the striation (modified from Xu et al., 2009). (b and c) Photographs showing the measured vertical separation of the trenches 1 and 5. S_{vm}: vertical separation.

I fully agree that the Yangsan fault is a Holocene active fault from the dating results. Overall, the trenches were not as effective as expected, with problems such as discontinuous deposition and less carbon-14 dating material. I suggest the authors carry out more detailed work and select a more suitable geomorphological location to excavate the paleoseismic trench in the future, providing the recurrence interval of the strong earthquakes.	Great suggestion. We are on the same boat with the reviewer on this matter. So, we have already added the limitations of our study to the conclusions. However, there exist much limitation in paleoseismic research in Korea. Rapid erosion rates and low deposition rates due to the humid climate, coupled with low tectonic activity relative to plate boundaries, make it difficult to recognize surface ruptures even if they occurred. Numerous cultivated fields and much human disturbance make trench site selection more difficult. It is also very difficult to obtain radiocarbon targets, and even if you can, there is a lot of room for misinterpretation due to tree root penetration in dense forests. So far, only one paleoseismic study in Korea has yielded a reliable radiocarbon age. In other words, Korea is the antithesis of arid regions with well-preserved surface rupture and regions of high tectonic activity. Given together, we believe that these difficulties make our research more valuable. Thank you again for your constructive comments.